Apocynum cannabinum や *Picrorhiza kurrora* などの植物の茎から分離、抽出された免疫調整物質であり、貪食細胞や非貪食細胞の NOX 活性を抑制することが報告されている（Stefanska and Pawliczak, 2008）。その抑制機序は完全には解明されていないが、$p47^{phox}$ の細胞膜への移行阻害と考えられており、H_2O_2 や MPO の作用により形成された APO ラジカル（APO の 2 量体を含む）が $p47^{phox}$ の thiol 基を酸化することによると考えられている。今回、APO による PBO の肝発がん促進効果が見いだせなかったが、グルタチオンやシステインなどのチオールの存在下では APO の作用が抑制されることが知られており、PBO によるグルタチオンの増加が NOX の効果発現に影響を及ぼした可能性が示唆された。PBO 投与ラットの肝臓におけるグルタチオン含量や GSH/GSSG の比率の検討はこれまでなされていないが、GSH の酸化酵素である *Gpx2* の mRNA レベルの増加が本実験やこれまでの研究で確認されている（Morita et al., 2013）。

APO は NOX 特異的な阻害剤であるが、NAC は一般的には抗酸化剤という区分に属する物質である。NAC はこれまでの報告では PPARα アゴニスト(CYP4A inducer)による肝発がん促進過程に対しては修飾作用を示さず(Nishimura et al., 2009)、CYP1A inducer（Indole-3-carbinol）には抑制効果を示していた(Shimamoto et al., 2011)。GST-P 陽性肝細胞巣を指標とした Indole-3-carbinol の肝発がん促進作用は NAC 併用処置により軽減されたものの、Cyp1A mRNA 発現レベルやミクロソームの ROS 産生、8-hydroxy-2'-deoxygunosine の発現レベルについての抑制効果は伴っておらず、Indole-3-carbinol についても CYP の誘導と肝発がん促進機構との関連性は明らかとなっていない。今回、CYP1A inducer である PBO 投与の肝臓において NAC 併用処置による修飾作用を見出せなかったことから、同種の薬物代謝酵素を誘導する薬剤においても発がん促進作用に関与する機序が異なる可能性が示唆された。

PBO 投与による NOX 関連遺伝子の発現が検出できなかった理由とし、PBO そのものが NOX 誘発性を有しなかった可能性に加え、標準的なラット二段階肝発がんモデルでは、試験系や観察期間を含め NOX 関連分子の変動をとらえることが難しかったことが挙げられる。従って、NOX の発現の高い肝内環境を設定するなどの実験系の改善が必要であると考えられる。NOX の関与する肝傷害として脂肪性肝疾患モデルが知られている。動物に高脂肪食を与えることで NOX の発現増加に伴って脂質過酸化が増加し（Matsunami et al., 2010）、APO 投与により肝脂肪化が軽減することが知られている（Lu et al., 2006）。高脂肪食摂取による脂肪肝は非アルコール性脂肪性肝疾患と呼ばれ、非アルコール性脂肪肝炎やそれに続く肝線維症を経て肝発がんにいたる進行性疾患として知られている（Sheedfar et al., 2013）。このような NOX 高発現環境下において被験物質の肝発がん性を検討することで、NOX の関与する肝発がん促進過程を明確化できる可能性が考えられる。次年度は、背景的に NOX の発現が高いことが示されている脂肪肝モデルを中期肝発がん性試験に適用し、NOX 高発現環境下において肝がん促進効果を検討する予定である。

E. 結論

肝発がん促進過程における NOX の関与をラット肝二段階発がんモデルを用いて検討したが、PBO の発がん促進過程においては NOX の関与を示唆する知見は得られなかった。

F. 健康危機情報

特になし

G. 研究発表

1. 論文発表

Morita, R., Yafune, A., Shiraki, A., Itahashi, M., Ishii, Y., Akane, H., Nakane, F., Suzuki, K., Shibutani, M., Mitsumori, K.: Liver tumor promoting effect of orphenadrine in rats and its possible mechanism of

action including CAR activation and oxidative stress. J. Toxicol. Sci. 38(3): 403-413, 2013.

Morita, R., Yafune, A., Shiraki, A., Itahashi, M., Akane, H., Nakane, F., Suzuki, K., Shibutani, M., Mitsumori, K.: Enhanced liver tumor promotion activity in rats subjected to combined administration of phenobarbital and orphenadrine. J. Toxicol. Sci. 38(3): 415-424, 2013.

2. 学会発表

盛田怜子, 八舟宏典, 赤根弘敏, 板橋　恵, 白木彩子, 鈴木和彦, 渋谷　淳, 三森国敏：Phenobarbital (PB) とPiperonyl butoxide (PBO) の併用投与によるラット肝発がんプロモーション作用の修飾に関する研究. 第40回日本毒性学会学術集会, 幕張, 第40回日本毒性学会学術集会講演要旨集：P-67, p.S300, 6月17-19日, 2013

盛田 怜子、林 仁美、勢川 理紗、鈴木 和彦、渋谷 淳、三森 国敏：CYP誘導剤の肝発がん促進作用に対する相互作用. 第28回発癌病理研究会、於沖縄、第28回発癌病理研究会プログラム：p. 34(演題19), 8月26-28日, 2013

Reiko Morita, Ayako Shiraki, Megu Itahashi, Kazuhiko Suzuki, Makoto Shibutani, Kunitoshi Mitsumori: Modification of Combined Administration of CYP Inducers in Rat Liver Tumor Promoting Activity. 11th European Congress of Toxicologic Pathology, Ghent, Belgium, P17, p.80, September 10–13, 2013

盛田怜子、白木彩子、板橋 恵、鈴木和彦、渋谷 淳、三森国敏：CYP誘導剤併用投与の肝発がん促進作用に対する影響. 第156回日本獣医学会, 岐阜, 第156回日本獣医学会学術集会講演要旨集：B65, p.223, 9月20-22日, 2013

H. 知的財産権の出願・登録状況

1. 特許取得

なし

2. 実用新案登録

なし

3. その他

なし

Table 1. Sequences of primers used for real-time RT-PCR

Gene	Forward sequence (5′–3′)	Reverse sequence (5′–3′)
Phase I drug metabolism enzymes		
Cyp1a1	GCCTTCACATCAGCCACAGA	TTGTGACTCTAACCACCCAGAATC
Cyp2b1/2	GGGACACTGAAAAAGAGTGAAGCT	AATGCCTTCGCCAAGACAAAT
Antioxidant enzymes		
Nqo1	GCTCTATCGTGCTCGCATGA	TCTTCTGTCACCCTGTGCTTGA
Gpx2	GTGTGATGTCAATGGGCAGAAT	AGGGCAGCTTGTCTTTCAGGTA
NOX-related factors		
Cybb	AAGAAGAAGGGATTCAGGATGGA	ACACTGCGGGACGCTTGA
Rac1	TCTCCTACCCGCAAACAGAC	CGGGTAGGTAATGGGAGTCA
Housekeeping gene		
Actb	CCCTGGCTCCTAGCACCAT	AGAGCCACCAATCCACACAGA

Table 2. Body and organ weights, daily food, water and estimated chemical intakes of rats given PBO, APO and/or NAC for 8 weeks after DEN initiation

Groups	DEN-alone	PBO	APO	NAC	PBO+APO	PBO+NAC
Number of rats	12	11	12	12	15	10
Final body weight (g)	279.9±13.9	205.1±7.4**	285.6±18.8	269.9±15.2	206.6±12.3**	194.6±14.7**
Food intake (g/rat/day)	12.7±0.9	11.7±2.4	12.9±1.0	12.1±1.1	11.7±2.5	11.5±2.6
Water intake (g/rat/day)	17.1±1.5	15.6±2.4	18.0±1.5	13.9±3.2	15.9±2.6	12.8±3.1
PBO intake (mg/kg BW/day)	–	37.63±2.15	–	–	37.28±2.77	35.45±2.82
APO intake (mg/kg BW/day)	–	–	0.95±0.08	–	0.64±0.06	–
NAC intake (mg/kg BW/day)	–	–	–	8.32±0.70	–	6.00±0.49
Absolute liver weight (g)	8.89±0.55	12.19±0.82**	8.96±0.75	8.94±1.25	12.61±1.21**	11.31±1.08**
Relative liver weight (% BW)	3.17±0.11	5.94±0.31**	3.13±0.08	3.32±0.54	6.10±0.43**	5.81±0.19**

Values are expressed as mean ± SD.

*$P < 0.05$ or **$P < 0.01$ compared with control group (Dunnett's or Steel's test).

Table 3. The result of blood biochemistry of rats given PBO, APO and/or NAC for 8 weeks after DEN initiation

Groups	DEN-alone	PBO	APO	NAC	PBO+APO	PBO+NAC
Number of rats	12	11	12	12	15	10
Total protein (g/dl)	6.62 ± 0.22	7.42 ± 0.21**	6.73 ± 0.26	6.72 ± 0.23	7.66 ± 0.36**	7.52 ± 0.30**
Albumin (g/dl)	4.73 ± 0.16	5.55 ± 0.18**	4.75 ± 0.13	4.74 ± 0.13	5.64 ± 0.14**	5.62 ± 0.19**
AST (GOT) (IU/l)	69.08 ± 5.05	60.64 ± 5.59*	69.50 ± 3.48	68.36 ± 4.06	61.71 ± 5.65*	59.00 ± 8.51*
ALT (GPT) (IU/l)	43.83 ± 4.15	43.55 ± 3.39	44.25 ± 4.37	45.58 ± 11.97	45.07 ± 3.38	44.20 ± 3.85
ALP (IU/l)	937.92 ± 70.30	951.00 ± 82.39	936.75 ± 84.79	1020.58 ± 249.03	972.07 ± 167.62	896.90 ± 74.38
Creatinin (mg/dl)	0.34 ± 0.05	0.30 ± 0.04	0.33 ± 0.05	0.32 ± 0.04	0.30 ± 0.00	0.29 ± 0.03
Urea nitrogen (mg/dl)	15.75 ± 1.48	22.36 ± 1.12**	15.83 ± 1.11	14.83 ± 1.03	21.27 ± 1.39**	23.50 ± 1.58**
Glucose (mg/dl)	192.75 ± 27.64	147.45 ± 17.87**	199.00 ± 34.47	176.50 ± 27.58	139.13 ± 21.54**	140.10 ± 18.45**
Triglyceride (mg/dl)	134.33 ± 25.00	30.91 ± 6.24**	112.33 ± 19.98	104.92 ± 22.66	38.93 ± 38.56**	24.60 ± 4.84**
Total cholesterol (mg/dl)	68.83 ± 3.13	103.18 ± 7.26**	74.67 ± 4.31*	78.67 ± 16.00*	110.40 ± 14.70**	111.10 ± 6.69**

Values are expressed as mean ± SD.

*$P < 0.05$ or **$P < 0.01$ compared with control group (Dunnett's or Steel's test).

Table. 4. GST-P-positive foci, and Ki-67 and TUNEL positive cell ratio in the liver of rats given PBO, APO and/or NAC for 8 weeks after DEN initiation

Groups	DEN-alone	PBO	APO	NAC	PBO+APO	PBO+NAC
Number of rats	12	11	12	12	15	10
GST-P positive foci						
Numbers (No./cm^2)	8.04± 2.53	23.79± 8.75**	7.97± 1.66	8.46± 2.15	17.82± 4.22**	17.85± 3.59**
Areas (mm^2/cm^2)	0.42± 0.14	1.82± 0.69**	0.42± 0.08	0.41± 0.12	1.66± 0.75**	1.75± 0.72**
Ki-67 positive cells (%)	4.89±0.55	12.19±0.82**	4.96±0.75	5.04±1.25	12.61±1.21**	11.31±1.08**
Caspase-3 positive cells (%)	1.17±0.11	3.94±0.31**	1.13±0.08	1.32±0.54	4.10±0.43**	3.81±0.19**

Values are expressed as mean ± S.D.

$^{**}P < 0.01$ compared with control group (Dunnett's or Steel's test).

Table 5. Changes of transcript expression in the liver of rats given PBO, APO and/or NAC for 8 weeks after DEN initiation

	Group					
Genes	DEN-alone	PBO	APO	NAC	PBO+APO	PBO+NAC
Drug metabolizing enzymes						
Cyp1a1	1.03±0.31	330.19±116.78**	1.02±0.33	1.19±0.64	352.45±104.01**	348.38±284.67**
Cyp2b1/2	1.03±0.29	298.74±21.86**	1.06±0.29	1.08±0.63	283.34±30.41**	279.17±39.42**
Antioxidant enzymes						
Nqo1	1.01±0.12	4.69±0.53**	1.08±0.10	1.20±0.29	6.93±1.68**	6.10±1.68**
Gpx2	1.03±0.27	45.58±5.81**	0.84±0.09	4.51±8.07	48.30±7.54**	40.31±7.23**
NOX-related factors						
Cybb	1.01±0.15	0.98±0.15	1.16±0.26	1.52±0.84	1.24±0.36	1.60±0.15
Rac1	1.01±0.13	1.01±0.04	1.01±0.07	1.13±0.20	0.99±0.16	1.04±0.13

Values of mRNA expression level (normalized by *Actb*) are expressed as mean ± S.D. (N=6).

**$P < 0.01$ compared with control group (Dunnett's or Steel's test).

別添５

研究成果の刊行に関する一覧表

書籍

著者氏名	論文タイトル名	書籍全体の編集者名	書　籍　名	出版社名	出版地	出版年	ページ
該当なし。							

雑誌

発表者氏名	論文タイトル名	発表誌名	巻号	ページ	出版年
Yafune, A., Taniai, E., Morita, R., Nakane, F., Suzuki, K., Mitsumori, K., Shibutani, M.	Expression patterns of cell cycle proteins in the livers of rats treated with hepatocarcinogens for 28 days.	Arch. Toxicol.	87(6)	1141-1153	2013
Yafune, A., Taniai, E., Morita, R., Hayashi, H., Suzuki, K., Mitsumori, K., Shibutani, M.	Aberrant activation of M phase proteins by cell proliferation-evoking carcinogens after 28-day administration in rats.	Toxicol. Lett.	219(3)	203-210	2013
Yafune, A., Taniai, E., Morita, R., Akane, H., Kimura, M., Mitsumori, K., Shibutani, M.	Immunohistochemical cellular distribution of proteins related to M phase regulation in early proliferative lesions induced by tumor promotion in rat two-stage carcinogenesis models.	Exp. Toxicol. Pathol.	66(1)	1-11	2014
Morita, R., Yafune, A., Shiraki, A., Itahashi, M., Ishii, Y., Akane, H., Nakane, F., Suzuki, K., Shibutani, M., Mitsumori, K.	Liver tumor promoting effect of orphenadrine in rats and its possible mechanism of action including CAR activation and oxidative stress.	J. Toxicol. Sci.	38(3)	403-413	2013
Morita, R., Yafune, A., Shiraki, A., Itahashi, M., Akane, H., Nakane, F., Suzuki, K., Shibutani, M., Mitsumori, K.	Enhanced liver tumor promotion activity in rats subjected to combined administration of phenobarbital and orphenadrine.	J. Toxicol. Sci.	38(3)	415-424	2013

研究成果の刊行物・別刷

Arch Toxicol (2013) 87:1141–1153
DOI 10.1007/s00204-013-1011-y

GENOTOXICITY AND CARCINOGENICITY

Expression patterns of cell cycle proteins in the livers of rats treated with hepatocarcinogens for 28 days

Atsunori Yafune · Eriko Taniai · Reiko Morita · Fumiyuki Nakane · Kazuhiko Suzuki · Kunitoshi Mitsumori · Makoto Shibutani

Received: 23 September 2012 / Accepted: 17 January 2013 / Published online: 15 February 2013

Abstract Some hepatocarcinogens induce cytomegaly, which reflects aberrant cell cycling and increased ploidy, from the early stages of administration to animals. To clarify the regulatory molecular mechanisms behind cell cycle aberrations related to the early stages of hepatocarcinogenesis, we performed gene expression analysis using microarrays and real-time reverse transcription polymerase chain reaction followed by immunohistochemical analysis in the livers of rats treated with the cytomegaly inducing hepatocarcinogens thioacetamide (TAA), fenbendazole, and methyleugenol, the cytomegaly non-inducing hepatocarcinogen piperonyl butoxide (PBO), or the non-carcinogenic hepatotoxicants acetaminophen and α-naphthyl isothiocyanate, for 28 days. Gene expression profiling showed that cell cycle-related genes, especially those of G_2/M phase, were mostly upregulated after TAA treatment. Immunohistochemical analysis was performed on cell cycle proteins that were upregulated by TAA treatment and on related proteins. All hepatocarcinogens, irrespective of their cytomegaly inducing potential, increased liver cells immunoreactive for $p21^{Cip1}$, which acts on cells arrested in G_1 phase, and for Aurora B or Incenp, which is suggestive of an increase in a cell population with chromosomal instability caused by overexpression. PBO did not induce cell proliferation after 28-day treatment. Hepatocarcinogens that induced cell proliferation after 28-day treatment also caused an increase in $p53^+$ cells in parallel with increased apoptotic cells, as well as increased population of cells expressing M phase-related proteins nuclear Cdc2, phospho-Histone H3, and HP1α. These results suggest that hepatocarcinogens may increase cellular populations arrested in G_1 phase or showing chromosomal instability after 28-day treatment. Hepatocarcinogens that induce cell cycle facilitation may cause M phase arrest accompanied by apoptosis.

Keywords Hepatocarcinogen · Cell cycle · Cytomegaly · Prediction marker

Abbreviations

ANIT	α-Naphthyl isothiocyanate
APAP	Acetaminophen
Cdc2	Cell division cycle 2
Cdk	Cyclin-dependent kinase
FB	Fenbendazole
HP1α	Heterochromatin protein 1α
Klf6	Kruppel-like factor 6
MEG	Methyleugenol
NDRG1	N-myc downstream regulated gene 1
p-Histone H3	Phosphorylated-Histone H3
PBO	Piperonyl butoxide
TAA	Thioacetamide
Topo IIα	Topoisomerase IIα

Electronic supplementary material The online version of this article (doi:10.1007/s00204-013-1011-y) contains supplementary material, which is available to authorized users.

A. Yafune · E. Taniai · R. Morita · F. Nakane · K. Suzuki · K. Mitsumori · M. Shibutani (✉)
Laboratory of Veterinary Pathology, Tokyo University of Agriculture and Technology, 3-5-8 Saiwai-cho, Fuchu-shi, Tokyo 183-8509, Japan
e-mail: mshibuta@cc.tuat.ac.jp

A. Yafune · E. Taniai · R. Morita
Pathogenetic Veterinary Science, United Graduate School of Veterinary Sciences, Gifu University, 1-1 Yanagido, Gifu-shi, Gifu 501-1193, Japan

A. Yafune
Gotemba Laboratory, Bozo Research Center Inc., 1284 Kamado, Gotemba, Shizuoka 412-0039, Japan

Introduction

The currently used methods for the evaluation of the carcinogenicity of chemicals are bioassays in which rodents are treated with the chemical for their entire 1.5- or 2-year life span. Long-term carcinogenicity studies using experimental animals are time-consuming, expensive, and involve the use of many animals. Medium-term carcinogenesis bioassays using rat liver or multi-organ models (Tamano 2010) or genetically modified animals using transgenic or gene targeting technologies (Eastin 1998) are used as alternative models. However, they are also expensive and time-consuming and often have limited target organs. Toxicogenomic approaches for prediction of carcinogenic potential in each target organ appear promising. Unfortunately, these are also expensive and require integrative methodologies between different laboratories sharing an expression database (Uehara et al. 2011). There is no commonly used rapid means of evaluating the carcinogenic potential of chemicals that can be used for genotoxic and non-genotoxic carcinogens. Therefore, it is essential to establish a short-term carcinogenicity screening system based on the molecular responses to the carcinogens in the target organs.

Evaluation of carcinogenicity study data collected in the National Toxicology Program (NTP) showed that prechronic liver lesions including hepatocellular necrosis, hepatocellular hypertrophy, hepatocellular cytomegaly, bile duct hyperplasia, and hepatocellular degeneration, along with increased liver weight in the prechronic studies may be used as components in the search for predictors of liver carcinogenicity in chronic 2-year bioassays (Allen et al. 2004). Some hepatocarcinogens induce cytomegaly characterized by the presence of hepatocytes with increased cytoplasmic volume and karyomegaly from the early stages of exposure (Allen et al. 2004; Hamadeh et al. 2004). The development of cytomegaly is suggestive of cell cycle aberrations causing chromosomal instability through nuclear division during mitosis. Mitotic aberrations such as chromosomal missegregation and cytokinesis failure occurring as a result of checkpoint dysfunction of the cell cycle can result in tetraploidy/aneuploidy (Ichijima et al. 2010).

Recent studies have shown that ochratoxin A, a renal carcinogen, can induce karyomegaly with DNA aneuploidy and polyploidy accompanied by abnormal expression of cell cycle proteins, especially G_2/M phase-related proteins (Adler et al. 2009). These cellular events may lead to chromosomal instability. Moreover, development of karyomegaly is also observed during carcinogenesis in the kidney and large intestine (Williams et al. 2002; Adler et al. 2009), suggesting a common mechanism for carcinogenesis across target organs. Therefore, we hypothesize that there is an early event in the carcinogenic response that causes the development of karyomegaly/cytomegaly by disrupting cell cycle regulation. We have previously analyzed cell cycle proteins in a study of 28-day repeated treatment with renal carcinogens to induce karyomegaly in rats (Taniai et al. 2012). We found that renal carcinogens, irrespective of karyomegaly inducing potential, increased the number of proximal tubular cells positive for Ki-67, a cell proliferation marker, and topoisomerase IIα (Topo IIα), suggesting that proliferation is accompanied by cell cycle aberration. These findings suggest that carcinogens may activate target cell proliferation after short-term repeated exposure.

In the present study, to further examine the regulatory molecular mechanisms behind cell cycle aberrations during the early stages of hepatocarcinogenesis, we first carried out global gene screening using microarrays in the liver of rats receiving repeated oral administration of thioacetamide (TAA), a representative cytomegaly inducing hepatocarcinogen, and then real-time reverse transcription polymerase chain reaction (RT-PCR) analysis in the livers of rats receiving TAA or fenbendazole (FB). We selected cell cycle-related genes based on the gene expression data. Localization of candidate proteins showing upregulation of mRNA and related proteins were further analyzed immunohistochemically in the livers of rats receiving the cytomegaly inducing hepatocarcinogens TAA, FB, and methyleugenol (MEG), the cytomegaly non-inducing hepatocarcinogen piperonyl butoxide (PBO), or the non-carcinogenic hepatotoxicants acetaminophen (APAP) and α-naphthyl isothiocyanate (ANIT) for 28 days.

Materials and methods

Chemicals

Thioacetamide (TAA; CAS No. 62-55-5, ≥98.0 %) and sterilized 0.5 % (w/v) methyl cellulose 400 solutions were purchased from Wako Pure Chemicals Industries (Osaka, Japan). Methyleugenol (MEG; CAS No. 93-15-2, >98.0 %), acetaminophen (APAP; CAS No. 103-90-2, ≥98.0 %), and α-naphthyl isothiocyanate (ANIT; CAS No. 551-06-4, ≥98.0 %) were purchased from Tokyo Chemical Industry Co. (Tokyo, Japan). Fenbendazole (FB; CAS No. 43210-67-9, ≥98.0 %) was purchased from LKT Laboratories, Inc (St. Paul, MN, USA), and piperonyl butoxide (PBO; CAS No. 51-03-6, ≥98.0 %) from Nagase & Co. (Osaka, Japan).

Animal experiments

Animals and experimental design were identical to those previously reported (Taniai et al. 2012). Animal studies were conducted in accordance with the institute Guide for Animal Experimentation, given free access to powdered

diets, and were maintained under standard conditions (room temperature, 23 ± 3 °C; relative humidity, 50 ± 20 %, 12-hour light/dark cycle). Briefly, 5-week-old male F344/NSIc rats (Japan SLC, Inc., Hamamatsu, Japan) were acclimatized to a powdered basal diet (Oriental Yeast Co., Tokyo, Japan) and tap water ad libitum for 1 week. Animals were randomized into groups of 10 animals and treated with TAA (400 ppm in the diet), FB (3,600 ppm in the diet), PBO (20,000 ppm in the diet), MEG (1,000 mg/kg body weight, daily by gavage), APAP (12,500 ppm in the diet), or ANIT. For ANIT, the initial dose was set at 1,000 ppm in the diet. However, as the general condition of the animals worsened, the dose was gradually reduced to 800 ppm for 14 days and 600 ppm for the following 7 days. TAA, FB, PBO, and MEG were selected as hepatocarcinogens/promoters in rats, and the dose levels of these compounds have shown to induce liver tumors or promote liver carcinogenesis in rats (Becker 1983; Takahashi et al. 1994; Shoda et al. 1999; NTP 2000; Ichimura et al. 2010). APAP and ANIT were selected as non-carcinogenic hepatotoxicants, and the dose of these compounds has shown to induce hepatotoxicity after 13- or 16-week administration in rats (Rees et al. 1962; NTP 1993). Ten untreated control animals were maintained on the basal diet and tap water without any treatment during the experimental period. One day after the 28-day treatment period, all animals were killed by exsanguination from the abdominal aorta under deep anesthesia and livers were removed.

Expression microarray analysis

Total RNA was extracted with the RNeasy Mini Kit (Qiagen, Hilden, Germany) according to the manufacturer's instructions. Using 10 μg of total RNA from one animal in the TAA-treatment group and one untreated control, double-stranded cDNA was synthesized with the Invitrogen Superscript Double-Stranded cDNA Synthesis Kit (Invitrogen Corp., Carlsbad, CA, USA), according to the manufacturer's protocol. The cDNA sample was labeled with Cy3 and loaded onto the *Rattus norvegicus* Roche NimbleGen microarray (Roche NimbleGen: Euk Expr 4x72k Catalog Arr, 26,208 targets; Roche Applied Science, Penzberg, Germany). Using the robust multiple average normalization method (Irizarry et al. 2003), differentially expressed genes were analyzed. Gene information was retrieved from the National Center for Biotechnology Information website (http://www.ncbi.nlm.nih.gov).

Real-time RT-PCR analysis

For confirmation of the microarray data, fluctuating transcript levels of representative cell cycle-related genes were subjected to mRNA expression analysis using the StepOnePlus™ Real-time RT-PCR System (Applied Biosystems Japan Ltd., Tokyo, Japan) with the SYBR® Green PCR Master Mix (Applied Biosystems Japan Ltd.). The forward and reverse primers listed in Table 1 were designed using the Primer Express 3.0 software (Applied Biosystems Japan Ltd.). Using the threshold cycle values of β-actin in the same sample as the endogenous control, the relative differences in gene expression were calculated using the $2^{-\Delta\Delta C_T}$ method (Livak and Schmittgen 2001).

Immunohistochemistry

Immunohistochemistry of liver sections was performed using the horseradish peroxidase avidin–biotin complex method using a VECTASTAIN® Elite ABC Kit (Vector Laboratories Inc., Burlingame, CA, USA), with the antibodies listed in Table 2 and 3,3'-diaminobenzidine/H_2O_2 as the chromogen. Antigen retrieval conditions for each antibody are shown in Table 2. Sections were counterstained with hematoxylin for microscopic examination.

Apoptosis assay

Liver sections were subjected to terminal deoxynucleotidyl transferase-mediated dUTP nick-end labeling (TUNEL) assay using the ApopTag® Peroxidase *In Situ* Apoptosis Detection Kit (Millipore, Billerica, MA, USA) according to the manufacturer's protocol. Briefly, deparaffinized sections were treated with 20 μg/ml proteinase K for 15 min at room temperature. Endogenous peroxidase activity was blocked with 3.0 % hydrogen peroxide. Color development and counter staining were as described in the immunohistochemistry section above.

Analysis of immunoreactivity

The immunostained cells were counted in 10 randomly selected areas per animal, avoiding portions of connective tissues and vasculature at a magnification of 200×. Immunoreactive liver cells were counted visually, and the total number of liver cells in the micrographs was separately counted using the image binarization method in the WinROOF image analysis and measurement software (version 6.4.2., Mitani Corporation, Fukui, Japan). The percentage of total immunoreactive cells in the 10 areas was estimated in each animal. A two-step screening system was applied for the analysis of antigen immunoreactivity in terms of cellular distribution in relation to carcinogen treatment. For first screening of proteins, livers from 5 animals per group were subjected to analysis. If a significant difference in the distribution of positive cells was observed between the untreated controls or non-carcinogens and carcinogens, the remaining 5 animals were similarly subjected to analysis for the second screening.

Table 1 Sequence of primers used for real-time RT-PCR analysis

Accession no.	Symbol	Forward primer[a]	Reverse primer
NM_130812	*Cdkn2b*	CCCTCACCAGACCTGTGCAT	CAGGCGTCACACACATCCA
NM_080782	*Cdkn1a*	ACCAGCCACAGGCACCAT	CGGCATACTTTGCTCCTGTGT
NM_171992	*Ccnd1*	GCGAGCCATGCTTAAGACTGA	CCCTCTGCACGCACTTGA
NM_053702	*Ccna2*	TGTCTCTGGTGGGTTGAGAAGA	ACCACAGCATGCCCAACAG
XM_001064075	*Ccne2*	TCTCCACAAGAAGCCCAGATAATT	GGTGATCTCCTCTGTTCTTTTTTTG
NM_001025682	*Cdr2*	CAAGGCCTCACAGCAGAAAATC	GAGGTGATCAATGTTGGTTTGC
NM_001012742	*Wee1*	CGGCAAACTCCTCAAGTGAATATT	CACTGTCCTGAGGAATGAAGCAT
NM_001107790	*Tpx2*	CCCAAGAGACCACCTGTTAAGC	ACTCTCGCTCATGAATTCGTTTCT
NM_024127	*Gadd45a*	CACCATAACTGTCGGCGTGTA	GGCACAGGACCACGTTGTC
NM_019296	*Cdk1*	GGTCGCCAGAGGTGTTGCT	TCTGCAAATATGGTCCCTATGCT
NM_171991	*Ccnb1*	TGTCCCACACGGAAGAATCTCT	GGCCACGGTTCACCATGA
NM_053749	*Aurkb*	CGGATGCATAATGAGATGGTAGAT	TCCCCACCATCAGTTCATAGC
NM_153296	*Aurka*	AAGAGAGTCATCCACAGAGACATCAA	CGATCTTCAACTCCCCATTTG
NM_030989	*Tp53*	CATGAGCGTTGCTCTGATGGT	GATTTCCTTCCACCCGGATAA
NM_001108099	*Mdm2*	GAAGGAGGACACACAAGACAAAGA	ATGGCTCGATGGCGTTCA
NM_001011991	*Ndrg1*	GTCACACCTTGTCTCCCATTATTG	CCAGGTGAGAGACATTCAGTTATCA
NM_031642	*Klf6*	GCGCCATCCAGTTTGCAT	GATCAGGAGTCGGAGCAGAAA
NM_031144	*Actb*	CCCTGGCTCCTAGCACCAT	AGAGCCACCAATCCACACAGA

Aurk aurora kinase, *Actb* actin beta, *Ccn* cyclin, *Cdk* cyclin-dependent kinase, *Cdkn* cyclin-dependent kinase inhibitor, *Cdr2* cerebellar degeneration-related 2, *Gadd45a* growth arrest and DNA-damage-inducible, alpha, *Klf6* Kruppel-like factor 6, *Mdm2* p53 binding protein homolog (mouse), *Ndrg1* N-myc downstream regulated 1, *RT-PCR* reverse transcription polymerase chain reaction, *Tp53* tumor protein p53, *Tpx2* microtubule-associated, homolog (*Xenopus laevis*), *Wee1* wee 1 homolog (*S. pombe*)

[a] The primer sets were designed using the Primer Express® software (Version 3.0; Applied Biosystems Japan Ltd.)

Table 2 Antibodies used in the present study

Antigen	Host species	Clonality	Dilution	Antigen retrieval[a]	Manufacturer (city, state, country)
Ki-67	Mouse	Monoclonal	1:50	Autoclaving	Dako (Glostrup, Denmark)
Cdc2 p34	Mouse	Monoclonal	1:100	None	Santa Cruz Biotechnology, Inc. (Dallas, TX, USA)
Histone H3 (Ser 10 phosphorylated)	Rabbit	Polyclonal	1:50	Autoclaving	Santa Cruz Biotechnology, Inc.
HP1α	Rabbit	Polyclonal	1:200	Microwaving	Cell Signaling Technology, Inc. (Danvers, MA, USA)
Aurora B	Rabbit	Polyclonal	1:200	None	Abcam (Cambridge, UK)
Incenp	Rabbit	Polyclonal	1:500	Autoclaving	Abcam
p53	Rabbit	Polyclonal	1:100	Autoclaving	Santa Cruz Biotechnology, Inc.
$p21^{Cip1}$	Mouse	Monoclonal	1:100	Microwaving	Abcam
$p27^{Kip1}$	Rabbit	Polyclonal	1:100	None	Cell Signaling Technology, Inc.
$p16^{Ink4a}$	Mouse	Monoclonal	1:100	None	Santa Cruz Biotechnology, Inc.
Wee1 (Ser 53 phosphorylated)	Rabbit	Polyclonal	1:100	Microwaving	Assay Biotechnology Co. Inc. (Sunnyvale, CA, USA)

[a] Antigen retrieval was applied to immunohistochemistry. Retrieval conditions were either autoclaving at 121 °C for 10 min or by microwaving at 90 °C for 10 min in 10 mM citrate buffer (pH 6.0)

Statistical analysis

Numerical data are represented as mean ± SD. All data were analyzed by the Bartlett's test for the homogeneity of variance. If there was no significant difference in variance, Dunnett's test was performed for comparison between the groups. If a significant difference was found in variance, Steel's test was performed. With regard to final body and

Table 3 Final body and liver weights of rats after 28-day treatment with hepatocarcinogens or hepatotoxicants

Group	No. of animals examined	Final body weight (g)	Liver weight	
			Absolute (g)	Relative (g/100 g BW)
Untreated controls	10	210±16[a]	7.93±0.87	3.68±0.17
TAA	10	141±13**	7.08±0.87*	4.94±0.24**
FB	10	208±14	8.62±0.68	4.04±0.14**
PBO	10	164±10**	11.89±0.77**	7.16±0.18**
MEG	10	175±13**	10.09±0.89**	5.68±0.31**
APAP	10	173±9**	7.17±0.55*	4.07±0.15**
ANIT	10	111±5**	6.43±0.44**	5.70±0.21**

* $P < 0.05$ versus untreated controls

** $P < 0.01$ versus untreated controls

[a] Mean ± SD

liver weights and real-time RT-PCR analyses, numerical data of the treatment groups were compared with those of the untreated controls. In case of the immunohistochemical analyses, numerical data were compared among all treatment groups and the untreated controls. Comparison between the APAP or ANIT and other treatment groups was similarly performed, excluding the untreated controls from comparison.

Results

Final body and liver weights

The final body and liver weights are shown in Table 3. As compared with the untreated controls, final body weights were significantly decreased in the TAA, PBO, MEG, APAP, and ANIT groups. The absolute liver weights of rats in the TAA, APAP, and ANIT groups were significantly lower than those of the untreated controls. The absolute liver weights of rats in the PBO and MEG groups were significantly higher than those of the untreated controls, but those of the FB group were not significantly changed. The relative liver weights of all treatment groups were significantly higher than those of the untreated controls.

Histopathological changes

Treatment with TAA induced diffuse liver cell cytomegaly often associated with anisokaryosis, aberrant mitosis, and apoptosis, as previously reported (Clawson et al. 1992). Bile duct proliferation and oval cell proliferation accompanied with mild interstitial fibrosis were evident in the periportal area. FB treatment induced centrilobular liver cell hypertrophy characterized by a marked increase in smooth endoplasmic reticulum, as previously reported (Shoda et al. 1999). Periportal liver cells showed cytomegaly associated with anisokaryosis and scattered mitoses. PBO treatment induced diffuse liver cell hypertrophy associated with cytoplasmic ground appearance and moderate nuclear enlargement, as previously reported (Muguruma et al. 2007). MEG treatment resulted in diffuse distribution of cytomegalic liver cells associated with anisokaryosis, as previously reported (NTP 2000). Centrilobular liver cell necrosis was also scattered. APAP treatment resulted in cytoplasmic eosinophilia and ground glass appearance of liver cells and ANIT treatment resulted in periportal bile duct proliferation, and scattered focal liver cell necrosis and microgranulomas, as previously reported (NTP 1993; Rees et al. 1962). However, neither APAP nor ANIT induced karyomegaly or cytomegaly in the liver cells.

Global gene expression changes after TAA treatment

Among the 26,208 gene targets identified in the microarray analysis, 2,888 genes showed altered expression in liver tissue after 28 days of TAA treatment compared to the untreated controls (1,681 genes were upregulated and 1,207 genes were downregulated, Online Resource 1). Most of the identified upregulated genes were related to cell proliferation, apoptosis, cell cycle, or intracellular signaling systems. Upregulated genes with apparent cell cycle function are listed in Table 4. The data discussed in this study have been deposited in NCBIs Gene Expression Omnibus (GEO, http://www.ncbi.nlm.nih.gov/geo/) and are accessible through GEO Series accession number GSE43066.

Real-time RT-PCR analysis

Expression levels of representative cell cycle-related genes selected from those listed in Table 4 were determined by real-time RT-PCR in the TAA and FB groups and compared with the untreated controls (Table 5). mRNA levels of all examined genes (*Cdkn2b, Cdkn1a, Ccnd1, Ccna2, Ccne2, Cdr2, Wee1, Tpx2, Gadd45a, Cdk1, Ccnb1, Aurkb,* and *Aurka*) were significantly increased in the TAA group as compared with the untreated controls. In addition, mRNA levels of *Cdkn2b, Cdkn1a, Ccnd1, Ccne2, Cdr2,* and *Cdk1* were also significantly increased in the FB group as compared with the untreated controls.

Cell proliferative activity and apoptosis

The nuclear antigen Ki-67 is a cell proliferation marker that is expressed in cells during the G_1 to M phase of the cell cycle (Scholzen and Gerdes 2000). The number of Ki-67$^+$ cells was significantly increased in the TAA, FB, and MEG groups as compared with the untreated controls, as previously reported (Taniai et al. 2012; Online Resource 2, Fig. s1A). A significant increase in Ki-67$^+$ cells was observed in the TAA and MEG groups as compared with the non-carcinogen groups (APAP and ANIT), while there was no difference in the number of Ki-67$^+$ cells in FB group compared with both non-carcinogen groups. PBO did not increase the number of Ki-67$^+$ proliferating cells.

TUNEL$^+$ cells were significantly increased in the TAA and MEG groups as compared with the untreated controls and non-carcinogen groups, as previously reported (Taniai et al. 2012; Online Resource 2, Fig. s1B). FB induced a significant increase in TUNEL$^+$ cells as compared with the APAP group. PBO did not increase the number of TUNEL$^+$ cells.

Immunoreactivity of G_1/S phase transition proteins

$p21^{Cip1}$ is a one of the Cyclin-dependent kinase (CDK) inhibitors that play a role in the G_1 checkpoint (Sherr and Roberts 1995). There was nuclear immunoreactivity for $p21^{Cip1}$ in the liver cells of untreated controls (Fig. 1a). The number of cells that was immunoreactive for $p21^{Cip1}$ was significantly increased in all carcinogen-treated groups as compared with the untreated controls and both non-carcinogen groups (Fig. 1a).

$p16^{Ink4a}$ and $p27^{Kip1}$, CDK inhibitors playing a role in the facilitation of the G_1 cell cycle arrest by binding to CDKs (Sherr and Roberts 1995), showed weak to moderate nuclear immunoreactivity in the liver cells of untreated controls. Strong nuclear and cytoplasmic immunoreactivity for $p16^{Ink4a}$ were found in the TAA group. Conversely, animals treated with other carcinogens or non-carcinogens only showed nuclear immunoreactivity. However, the number of immunoreactive cells was mostly unchanged by these treatments (Online Resource 2, Fig. s2A). The number of $p27^{Kip1+}$ cells did not statistically change in any of the carcinogen groups as compared with the untreated controls and non-carcinogen groups (Online Resource 2, Fig. s2B).

Immunoreactivity of G_2/M transition proteins

Cdc2, a molecule that drives the G_2/M transition in coordination with cyclin B1 (Chan et al. 1999), showed nuclear and/or cytoplasmic immunoreactivity in the liver cells of the untreated controls with the antibody recognizing both the phosphorylated and non-phosphorylated isoforms used here. Because Cdc2 is transported into the nucleus together with cyclin B1 upon activation (Chan et al. 1999), we counted cells showing nuclear immunoreactivity. Expression of nuclear Cdc2$^+$ cells significantly increased in the TAA, FB, and MEG groups as compared with the untreated controls and both non-carcinogen groups. However, PBO did not increase the number of nuclear Cdc2$^+$ cells (Fig. 1b).

Phospho-Wee1, acting at the G_2/M transition (Hashimoto et al. 2006), showed weak-to-moderate nuclear immunoreactivity in the liver cells of untreated controls. However, there were no specific expression changes in response to carcinogen treatment as compared with untreated controls or non-carcinogen groups (Online Resource 2, Fig. s2C).

Immunoreactivity of M phase proteins

Aurora B and Incenp, an interaction partner during mitosis (Ruchaud et al. 2007), were immunolocalized in the nuclei of the liver cells of untreated controls. Aurora B-immunoreactive cells were significantly increased in all carcinogen groups as compared with the untreated controls and the APAP group. In comparison with the ANIT group, Aurora B-immunoreactive cells significantly increased after treatment with FB, PBO, and MEG (Fig. 1c). Incenp-immunoreactive cells were significantly increased in all carcinogen groups as compared with the untreated controls and the ANIT group. However, APAP significantly increased Incenp$^+$ cells similar to the carcinogen groups (Fig. 1d). Phosphorylated-Histone H3 (p-Histone H3), the phosphorylated active isoform by Aurora B-kinase activity, causes heterochromatin protein 1α (HP1α) dissociation from heterochromatin, both acting at the early M phase (Hirota et al. 2005). Both p-Histone H3 and HP1α showed nuclear immunolocalization in the untreated controls. p-Histone H3$^+$ cells were significantly increased in the carcinogen groups as compared with the untreated controls and the APAP group. In comparison with the ANIT group, p-Histone H3 immunoreactive cells were significantly increased in the TAA, FB, and MEG groups (Fig. 1e). The number of HP1α$^+$ cells was significantly increased in the TAA, FB, and MEG groups as compared with the untreated controls. A significant increase in HP1α$^+$ cells was observed in the TAA and MEG groups as compared with the non-carcinogen groups, while the number of HP1α$^+$ cells in the FB group was statistically not different from those of the non-carcinogen groups. PBO did not increase HP1α$^+$ cells (Fig. 1f).

Expression of p53 and downstream Mdm2

Tp53 mRNA levels were significantly increased in the TAA group as compared with the untreated controls.

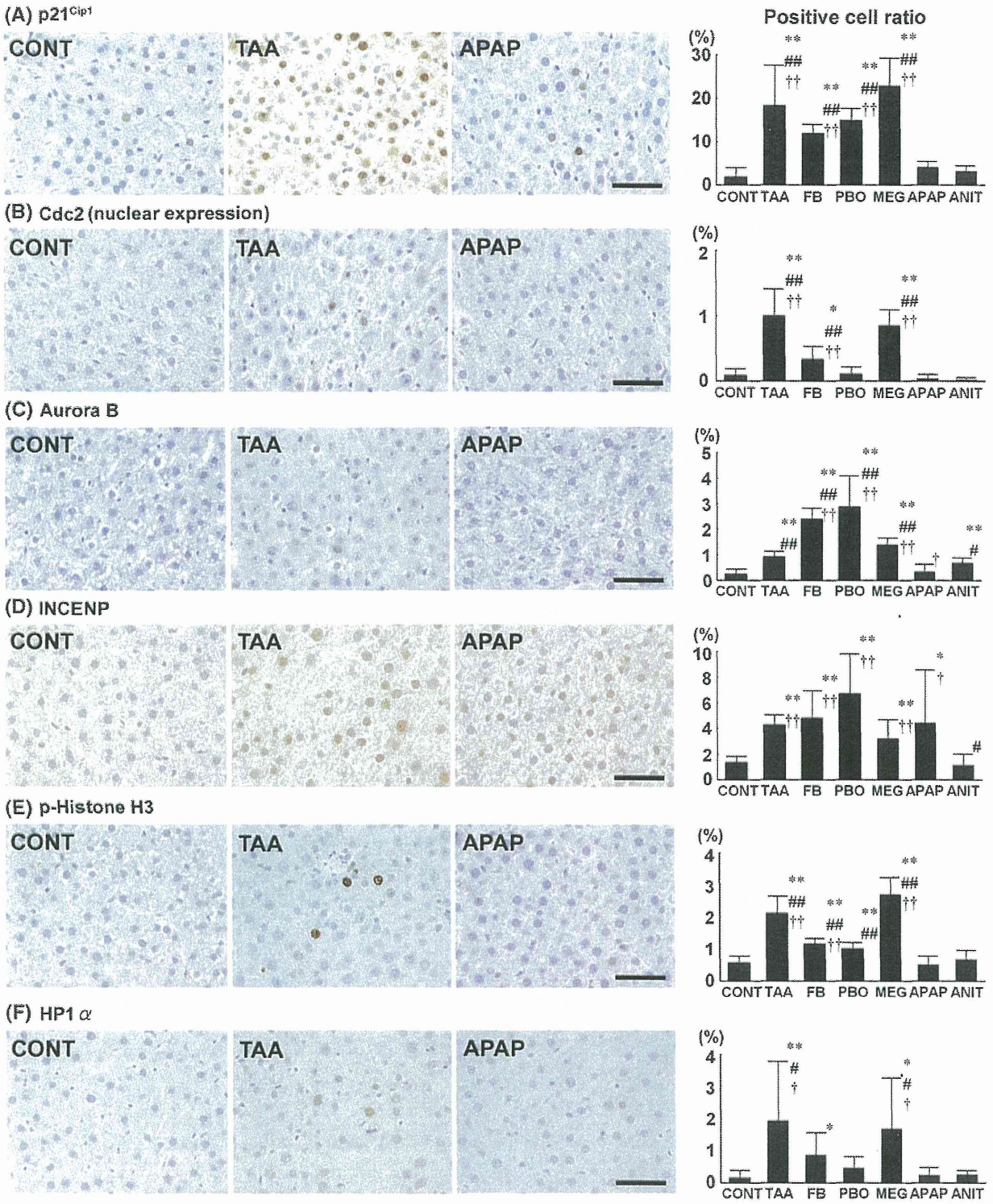

Fig. 1 Immunohistochemical cellular distribution of cell cycle proteins in liver cells after 28-day treatment with hepatocarcinogens or non-carcinogens in rats. Photomicrographs show distributions of $p21^{Cip1}$, nuclear Cdc2, Aurora B, Incenp, p-Histone H3, and HP1α immunoreactive cells in the livers of representative cases of an untreated control and animals treated with TAA or APAP. The graphs show positive cell ratios (%) of liver cells per total cells counted using 10 animals in each group. Values are presented as mean + SD (**a**) $p21^{Cip1}$, (**b**) Cdc2, (**c**) Aurora B, (**d**) Incenp, (**e**) p-Histone H3, and (**f**) HP1α. Magnification: ×400 (*Bar* = 50 μm). *, ** $P < 0.05$, 0.01 versus untreated controls (Dunnett's or Steel's test). #, ## $P < 0.05$, 0.01 versus APAP (Dunnett's or Steel's test). †, †† $P < 0.05$, 0.01 versus ANIT (Dunnett's or Steel's test)

Table 4 Representative cell cycle-related genes with known functional annotations that were upregulated in the livers of rats treated with TAA (≥twofold)

Accession No.	Gene title	Symbol	TAA
XM_001054052	Anaphase promoting complex subunit 4	Anapc4	2.30
NM_153296	Aurora kinase A	Aurka	2.22
NM_053749	Aurora kinase B	Aurkb	4.03
XM_001080790	Cancer susceptibility candidate 5	Casc5	2.71
NM_053702	Cyclin A2	Ccna2	2.26
NM_171991	Cyclin B1	Ccnb1	4.16
NM_001009470	Cyclin B2	Ccnb2	2.45
NM_171992	Cyclin D1	Ccnd1	2.54
XM_001077331	Cyclin E1	Ccne1	3.80
XM_001064075	Cyclin E2	Ccne2	3.94
NM_012923	Cyclin G1	Ccng1	6.18
NM_019296	Cyclin-dependent kinase 1	Cdc2	2.52
XM_001068286	Cell division cycle associated 2	Cdca2	5.10
NM_001007648	Cell division cycle associated 3	Cdca3	2.93
NM_001025693	Cell division cycle associated 7	Cdca7	7.72
NM_001025050	Cell division cycle associated 8	Cdca8	2.92
NM_001012035	Cyclin-dependent kinase-like 2 (CDC2-related kinase)	Cdkl2	2.06
NM_080782	Cyclin-dependent kinase inhibitor 1A	Cdkn1a	5.96
NM_130812	Cyclin-dependent kinase inhibitor 2B (p15, inhibits CDK4)	Cdkn2b	2.52
NM_001025682	Cerebellar degeneration-related 2	Cdr2	5.90
XM_001069485	Centromere protein A	Cenpa	2.72
XM_001077739	Centromere protein E	Cenpe	2.78
NM_001008366	Centromere protein N	Cenpn	3.60
NM_001014215	Centromere protein Q	Cenpq	2.28
NM_001025646	Centrosomal protein 55	Cep55	2.20
NM_001017470	Centrosomal protein 70	Cep70	2.88
XM_001067027	Centrosomal protein 76	Cep76	3.34
XM_001076228	Centrosomal protein 135	Cep135	2.58
NM_080400	CHK1 checkpoint homolog (S. pombe)	Chek1	2.60
XM_001058264	Claspin homolog (Xenopus laevis)	Clspn	2.29
XM_001073486	Disks, large (Drosophila) homolog-associated protein 5	Dlgap5	2.68
XM_001070442	Excision repair cross-complementing rodent repair deficiency complementation group 6-like	Ercc6 l	2.11
XM_001067790	Extra spindle poles like 1 (S. cerevisiae)	Espl1	2.30
XM_001065873	F-box protein 5	Fbxo5	2.06
XM_001075601	Fizzy/cell division cycle 20 related 1 (Drosophila)	Fzr1	2.20
NM_024127	Growth arrest and DNA-damage-inducible, alpha	Gadd45a	2.54
NM_001008321	Growth arrest and DNA-damage-inducible, beta	Gadd45b	2.73
XM_001078275	G-2 and S-phase expressed 1	Gtse1	14.53
XM_001074188	Inner centromere protein	Incenp	3.37
XM_001065116	Kinesin family member 2A	Kif2a	4.79
NM_001085369	Kinesin family member 2C	Kif2c	2.10
XM_001061764	Kinesin family member 20A	Kif20a	2.43
XM_001070728	Minichromosome maintenance complex component 3	Mcm3	2.94
XM_001068436	Similar to mcdc21 protein; minichromosome maintenance complex component 4	Mcm4	2.50
NM_012603	Myelocytomatosis oncogene	Myc	3.30
XM_001055166	NIMA (never in mitosis gene a)-related expressed kinase 2	Nek2	2.07
NM_182953	NIMA (never in mitosis gene a)-related kinase 6	Nek6	2.34
NM_177931	Origin recognition complex, subunit 1-like (yeast)	Orc1 l	2.10

Table 4 continued

Accession No.	Gene title	Symbol	TAA
NM_199092	Origin recognition complex, subunit 4-like (yeast)	Orc4 l	2.53
NM_001033690	Origin recognition complex, subunit 6 like (yeast)	Orc6 l	2.19
NM 017198	p21 protein (Cdc42/Rac)-activated kinase 1	Pak1	2.90
NM_017100	Polo-like kinase 1 (Drosophila)	Plk1	3.24
NM_031821	Polo-like kinase 2 (Drosophila)	Plk2	3.41
NM_001007754	Ras association (RalGDS/AF-6) domain family member 1	Rassf1	2.43
XM_001055763	Retinoblastoma-like 1 (p107)	Rbl1	2.60
XM_001077474	SPC24, NDC80 kinetochore complex component, homolog (S. cerevisiae)	Spc24	4.70
NM_001009654	SPC25, NDC80 kinetochore complex component, homolog (S. cerevisiae)	Spc25	5.73
NM_022183	Topoisomerase (DNA) II alpha	Top2a	2.20
NM_001107790	TPX2, microtubule-associated, homolog (Xenopus laevis)	Tpx2	3.18
NM_001012742	Wee 1 homolog (S. pombe)	Wee1	6.38
NM_019376	Tyrosine 3-monooxygenase/tryptophan 5-monooxygenase activation protein, gamma polypeptide	Ywhag	2.30

Values are fold change with the expression level in the untreated control group set as 1

mRNA levels of *Mdm2*, a protein regulated by *Tp53*, were significantly increased in both TAA and FB groups as compared with the untreated controls (Fig. 2a).

Immunohistochemically, p53 showed nuclear immunolocalization in the untreated controls. Immunoreactive cells for p53 were significantly increased in the TAA, FB, and MEG groups as compared with the untreated controls and the non-carcinogen groups (Fig. 2b). However, PBO did not increase the number of $p53^+$ cells.

Real-time RT-PCR analysis of Ndrg1 and Klf6

Gene expression levels of N-myc downstream regulated gene 1 (*Ndrg1*) and Kruppel-like factor 6 (*Klf6*) were investigated in all hepatocarcinogen groups and compared with those of the untreated controls (Fig. 3). Transcript levels of *Ndrg1* significantly increased in the TAA group as compared with the untreated controls. Transcript levels of *Klf6* significantly increased in the TAA, PBO, and MEG groups as compared with the untreated controls. Transcript levels of *Klf6* were also non-significantly increased in the FB group (Fig. 3).

Discussion

We used microarrays to profile gene expression in the livers of rats treated with TAA for 28 days and found fluctuations in transcript levels of cell cycle-related genes. We then investigated the immunohistochemical cellular distribution of cell cycle proteins and reviewed the results along with the cell proliferation activity and apoptotic cell distribution that we previously studied in the livers of rats treated with hepatocarcinogens or non-hepatocarcinogenic hepatotoxicants (Taniai et al. 2012). We found that all hepatocarcinogens studied, irrespective of their cytomegaly inducing potential, increased cellular distribution of the G_1/S checkpoint protein $p21^{Cip1}$ and of the M phase proteins Aurora B and Incenp. We also found that hepatocarcinogens that induced high cell proliferation activity by increasing the number of $Ki\text{-}67^+$ cells induced increases in the cellular distribution of p53 and the M phase-related proteins nuclear Cdc2, p-Histone H3, and HP1α. These results suggest that hepatocarcinogens increased cell populations in the G_1/S checkpoint or M phase, and hepatocarcinogens that induced high cell proliferation activity also increased cell populations facilitating M phase arrest.

Repeated treatment of rats with chemical carcinogens often results in target cell proliferation (Tanaka et al. 2000; Lock and Hard 2004). We recently found that carcinogens that caused high cell proliferation activity, irrespective of the target organ, increased the population of cells co-expressing Topo IIα and ubiquitin D (Ubd) (Taniai et al. 2012). Topo IIα functions at the G_2/M transition (Wang et al. 2008), and overexpression of Ubd leads to chromosomal instability through reduction of kinetochore localization of the spindle assembly checkpoint protein Mad2 (Lim et al. 2006; Herrmann et al. 2007). In the present study, we found an increase in nuclear Cdc2-expressing liver cells similar to that of $Ki\text{-}67^+$ cells after treatment with three of the four hepatocarcinogens (TAA, FB and MEG). Cdc2 and cyclin B form the cyclin B-Cdc2 complex, which initiates the G_2/M transition, and nuclear localization of Cdc2 represents the active isoform entering at the M phase (Kawamoto et al. 1997; Chan et al. 1999). We previously found an increase in $Cdc2^+$ cells parallel to that of $Ki\text{-}67^+$ cells in the proliferative lesions in a

Table 5 Validations in transcript levels measured by real-time RT–PCR in the livers of rats treated with TAA or FB

Gene symbol	Real-time RT-PCR normalized by *Actb*	
	TAA[a]	FB[a]
Cdkn2b	4.32 ± 0.20[b]**	2.03 ± 0.57**
Cdkn1a	3.49 ± 1.02**	2.32 ± 0.69**
Ccnd1	2.73 ± 0.52**	1.79 ± 0.48*
Ccna2	3.06 ± 0.61**	1.56 ± 0.52
Ccne2	6.60 ± 2.11**	1.48 ± 0.33*
Cdr2	7.94 ± 2.01**	1.44 ± 0.25*
Wee1	4.99 ± 2.83*	1.18 ± 0.54
Tpx2	3.38 ± 0.28**	1.16 ± 0.28
Gadd45a	2.76 ± 0.80**	1.60 ± 0.62
Cdk1	2.69 ± 0.61**	1.64 ± 0.44*
Ccnb1	2.28 ± 0.59**	1.57 ± 0.50
Aurkb	2.75 ± 0.65**	1.34 ± 0.21
Aurka	2.85 ± 0.42**	1.27 ± 0.27

Aurk aurora kinase, *Ccn* cyclin, *Cdk* cyclin-dependent kinase, *Cdkn* cyclin-dependent kinase inhibitor, *Cdr2* cerebellar degeneration-related 2, *Gadd45a* growth arrest and DNA-damage-inducible, alpha, *Tpx2* microtubule-associated, homolog (*Xenopus laevis*), *Wee1* wee 1 homolog (*S. pombe*)

* $P < 0.05$ versus untreated controls

** $P < 0.01$ versus untreated controls

[a] Numbers of animals examined were 6 in each group

[b] Mean ± SD

two-stage thyroid carcinogenesis model, suggestive of cell proliferation activity (Ago et al. 2010). We also found an increased number of cells positive for p-Histone H3 and its interaction partner HP1α, acting at the early M phase (Hirota et al. 2005), after treatment with hepatocarcinogens that induce high cell proliferation activity. The only exception was an increase in p-Histone $H3^+$ cells after treatment with PBO without increased cell proliferation. It was previously reported that p-Histone H3 and HP1α reflect cell proliferation (De Koning et al. 2009; Aune et al. 2011). Together with our previous study results, these results suggest that carcinogens inducing high cell proliferation activity produce cell populations undergoing sustained activation of the G_2/M checkpoint, resulting in cells inappropriately exiting from the G_2/M checkpoint and undergoing M phase arrest.

Like nuclear Cdc2, p-Histone H3 and HP1α, Aurora B and its interaction partner Incenp are M phase proteins. The Aurora B-Incenp complex has a function in correcting chromosome attachments (Ruchaud et al. 2007). We found that all hepatocarcinogens studied increased the number of Aurora B^+ or $Incenp^+$ cells, irrespective of the potential for inducing cell proliferation, as compared with the untreated controls and non-carcinogenic APAP and ANIT. The exception was an increase in the $Incenp^+$ population caused by APAP. Overexpression of Aurora B causes chromosomal instability in various cancer cells (Qi et al. 2007). It was reported that aberrant expression of Incenp may cause chromosomal instability or its aberrant segregation in human breast cancer cells (Nguyên and Ravid 2006). Therefore, hepatocarcinogens may cause chromosomal instability at the early stages of hepatocarcinogenesis and hepatocarcinogens that induce cell proliferation further produce cells in M phase arrest.

In the present study, $p21^{Cip1+}$ cells specifically increased after treatment with hepatocarcinogens. We did not find fluctuations in immunoreactive cellular distribution of other CDK inhibitors such as $p16^{Ink4a}$ and $p27^{Kip1}$ specific to hepatocarcinogens. Expression of $p21^{Cip1}$ is usually regulated by p53 to mediate G_1 arrest (Sherr and Roberts 1995). While the cellular distribution pattern of $p21^{Cip1}$ was similar to that of p53 after treatment with TAA, FB, and MEG, p53 did not respond to PBO in the present study. It is reported that there are a number of p53-independent mechanisms for $p21^{Cip1}$ induction (Abbas and Dutta 2009). There are a number of p53-independent $p21^{Cip1}$ inducers, such as Ndrg1 and Klf6 (Abbas and Dutta 2009; Kovacevic et al. 2011). In the present study, expression of both *Ndrg1* and *Klf6* was found to be upregulated by TAA-treatment, as shown by microarray analysis. We further found upregulation of *Klf6* by three of the four hepatocarcinogens (TAA, PBO and MEG) by real-time RT-PCR analysis as compared with untreated control animals. Therefore, it is possible that 28-day treatment with hepatocarcinogens produces cell populations arrested at the G_1 phase by $p21^{Cip1}$ via a mechanism independent of p53.

In the present study, transcript levels of *p53* and *Mdm2* significantly increased in the TAA group. $p53^+$ cells were increased after treatment with hepatocarcinogens that induced cell proliferation. It is well known that p53 induces apoptosis in response to DNA damage (Gotz and Montenarh 1995). We previously demonstrated that hepatocarcinogens that induced cell proliferation also induce apoptosis of liver cells (Taniai et al. 2012). These results suggest that hepatocarcinogens that induce cell proliferation also activate the p53 signaling cascade in response to G_1 or M phase arrest to undergo apoptosis. An increase in Mdm2 transcripts may represent facilitation of metabolic turnover of p53 (Fuchs et al. 1998).

With regard to the difference in the cellular responses on M phase proteins between PBO and other hepatocarcinogens, we think cellular responses may be parallel to the cell proliferation potential of carcinogens. It has been proposed that a non-genotoxic mode of action to induce hepatocellular apoptosis with subsequent regeneration (proliferation) is responsible for the hepatocarcinogenicity of fumonisin B_1 mycotoxin (Dragan et al. 2001). We recently found increased proliferation and apoptosis of liver cells

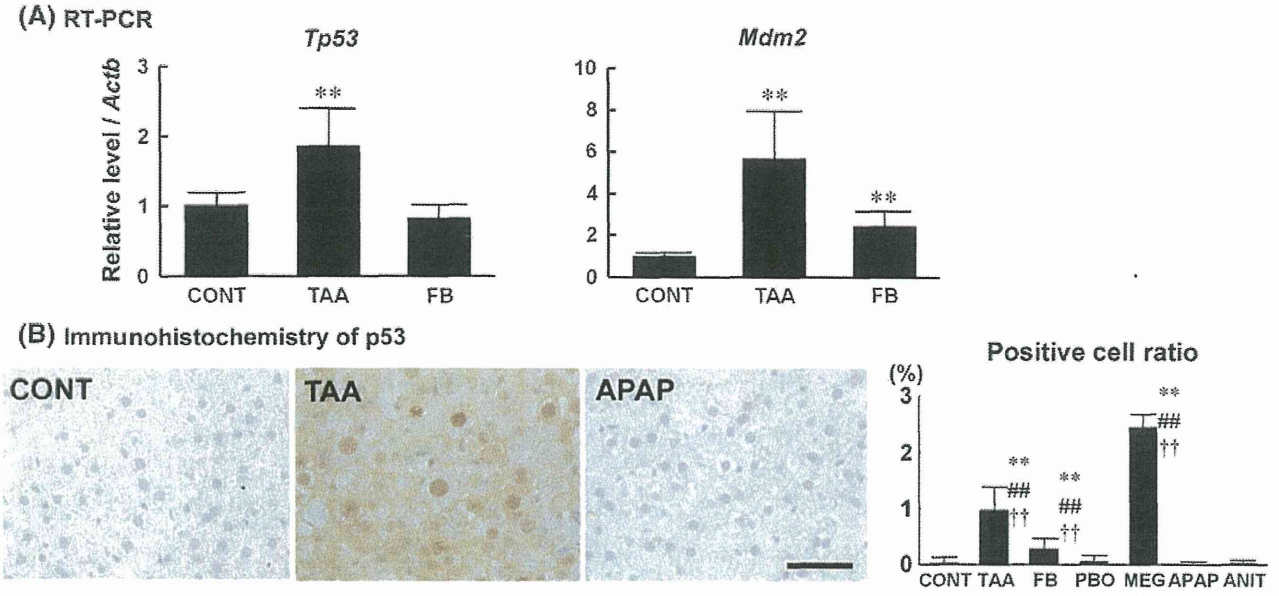

Fig. 2 Expression of p53 and downstream Mdm2 in the liver after 28-day treatment with hepatocarcinogens in rats. **a** Real-time RT-PCR analysis of p53 and Mdm2. Values are expressed as group mean fold changes over untreated controls. Values represent mean + SD *, ** $P < 0.05$, 0.01 versus untreated controls (Dunnett's or Steel's test). **b** Immunohistochemical cellular distribution of p53 in liver cells. Photomicrographs show immunoreactive cell distributions of p53 in the liver cells in representative cases of an untreated control and animals treated with TAA or APAP. The graphs show positive cell ratios (%) of liver cells per total cells counted using 10 animals in each group. Magnification: ×400 (*Bar* = 50 μm). ** $P < 0.01$ versus untreated controls (Dunnett's or Steel's test). ## $P < 0.01$ versus APAP (Dunnett's or Steel's test). †† $P < 0.01$ versus ANIT (Dunnett's or Steel's test)

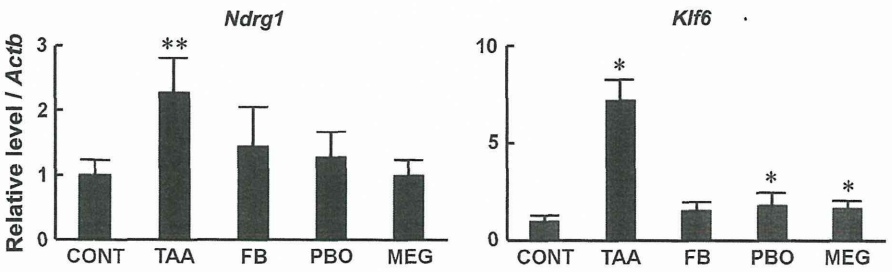

Fig. 3 Real-time RT-PCR analysis of *Ndrg1* and *Klf6*. Values are expressed as group mean fold changes over untreated controls. Numbers of animals examined were 6 in each group. Values represent mean + SD *, ** $P < 0.05$, 0.01 versus untreated controls (Dunnett's or Steel's test)

following treatment with either TAA, FB, or MEG; however, we did not find increased proliferation or apoptosis after PBO treatment (Taniai et al. 2012). It may be reasonable to hypothesize that induction of proliferation and apoptosis in carcinogenic target cells is dependent on carcinogenic potential of chemicals administered. It is well known that tumor-promoting potential of hepatocarcinogens in a rat two-stage hepatocarcinogenesis model correlates well with their hepatocarcinogenic potential (Shirai 1997). We previously reported that TAA and FB had higher tumor promoting activity than PBO (Ichimura et al. 2010), with the dose level used in the present study. MEG induces hepatocellular adenomas and carcinomas in rats after repeated oral administration at 300 mg/kg/day even at the one-year interim killing in two-year carcinogenesis test (NTP 2000). This dose is less than one-third of the dose level in the present study. Therefore, the lack of cellular responses to some M phase proteins with PBO may be a reflection of its weaker carcinogenic potential as compared with TAA, FB, and MEG.

In conclusion, hepatocarcinogens, irrespective of their cytomegaly inducing potential, increased the population of $p21^{Cip1+}$ cells, suggesting production of a cell population arrested at the G_1 phase by $p21^{Cip1}$. All hepatocarcinogens studied also increased Aurora B^+ and $Incenp^+$ cells, suggesting an increased cell population with chromosomal instability. Hepatocarcinogens that induced cell proliferation further increased the number of immunoreactive cells for p53, nuclear Cdc2, p-Histone H3, and HP1α, suggesting that cell cycle facilitation may cause M phase arrest accompanied by apoptosis. Therefore, the present study indicates that a combination of these proteins may be an early prediction marker of hepatocarcinogens in a 28-day treatment scheme in rats.